The impact of the Kasatochi eruption on the Moon's illumination during the August 2008 lunar eclipse

A. García Muñoz,[1,2] E. Pallé,[1,2] M. R. Zapatero Osorio,[3] and E. L. Martín[3]

Received 29 April 2011; revised 2 June 2011; accepted 10 June 2011; published 21 July 2011.

[1] The Moon's changeable aspect during a lunar eclipse is largely attributable to variations in the refracted unscattered sunlight absorbed by the terrestrial atmosphere that occur as the satellite crosses the Earth's shadow. The contribution to the Moon's aspect from sunlight scattered at the Earth's terminator is generally deemed minor. However, our analysis of a published spectrum of the 16 August 2008 lunar eclipse shows that diffuse sunlight is a major component of the measured spectrum at wavelengths shorter than 600 nm. The conclusion is supported by two distinct features, namely the spectrum's tail at short wavelengths and the unequal absorption by an oxygen collisional complex at two nearby bands. Our findings are consistent with the presence of the volcanic cloud reported at high northern latitudes following the 7–8 August 2008 eruption in Alaska of the Kasatochi volcano. The cloud both attenuates the unscattered sunlight and enhances moderately the scattered component, thus modifying the contrast between the two contributions.
Citation: García Muñoz, A., E. Pallé, M. R. Zapatero Osorio, and E. L. Martín (2011), The impact of the Kasatochi eruption on the Moon's illumination during the August 2008 lunar eclipse, *Geophys. Res. Lett.*, *38*, L14805, doi:10.1029/2011GL047981.

1. Introduction

[2] The classical theory of lunar eclipses accounts for refraction, differential absorption and focusing to explain the Moon's aspect during an eclipse [*Link*, 1962]. Link's classical theory has been subsequently perfected and used to investigate the composition and aerosol loading of the Earth's atmosphere [e.g., *Ugolnikov and Maslov*, 2008]. Aerosols play a critical role in the interpretation of lunar eclipses as their content, distribution and optical properties are largely unpredictable. Volcanic eruptions and meteor showers are two natural sources of aerosols with the potential for perturbing the atmosphere and, in turn, the aspect of the eclipsed Moon [*Keen*, 1983; *Vollmer and Gedzelman*, 2008]. Occasionally, large wildfires may also perturb the atmosphere [*Fromm et al.*, 2010].

[3] *García Muñoz and Pallé* [2011] have revisited the lunar eclipse theory and estimated the impact of volcanic aerosols on the spectrum of sunlight at the eclipsed Moon. Aerosols may substantially attenuate the direct sunlight while simultaneously enhancing somewhat the scattered contribution. The latter depends strongly on the capacity of aerosols for forward-scattering the incident light and, consequently, on the aerosols' size. The spectroscopic characterization of the sunlight reflected from the eclipsed Moon takes the investigation of lunar eclipses farther than allowed for by photometry and the traditional color indices.

[4] The 7–8 August 2008 eruption of the Kasatochi volcano (52.17°N, 175.51°W, Aleutian Islands, Alaska) ended a period of global low stratospheric aerosol amounts. The three main explosions recorded over two days plus the release of gas that followed for hours delivered into the atmosphere ~1.5 Tg of SO_2 [*Waythomas et al.*, 2010], which is ~30 times less than the SO_2 injected by Pinatubo in 1991. The plume of gas and ash rose up to ~14–18 km and drifted eastward carried by jet winds, spreading rapidly over North America, Greenland, and the North Atlantic Ocean. The cloud was spotted above Europe on 15 August, one week after the eruption [*Martinsson et al.*, 2009].

[5] Our paper shows that a published spectrum of the Moon in umbra during the August 2008 lunar eclipse contains sunlight scattered at the Earth's terminator. We argue that the Kasatochi eruption is the most plausible origin for the abnormally elevated atmospheric opacity needed to explain the observation. *Vidal-Madjar et al.* [2010] have published a spectrum of the August 2008 lunar eclipse, but covering only the penumbra.

2. Data

[6] We use data of the 16 August 2008 lunar eclipse obtained with the ALFOSC instrument mounted on the Nordic Optical Telescope at the Observatorio del Roque de los Muchachos (La Palma, Spain) and presented by *Pallé et al.* [2009]. The dataset comprises spectra of the Moon in umbra (21:36UT), penumbra (22:11UT), and out of eclipse (23:09UT). *Pallé et al.* [2009] derived a lunar eclipse spectrum from the ratio of umbra and penumbra spectra. The ratio cancels out the solar spectrum and the telluric signature of the Moon-to-telescope optical path. What remains is the imprint of the limb-viewed terrestrial atmosphere (averaged in a particular way over the terminator) on the sunlight that reaches the Moon in umbra. Our analysis sets out from the 400–900 nm published spectrum.

[7] The solar elevation angle, e, is the geocentric angle between the incident sunbeam direction and the direction from the Earth's centre to the lunar disk parcel targeted by the telescope. We have that $e \sim 0.34°$ for the slit projected on the Moon. The structure of an umbra spectrum is very sensitive to e [*García Muñoz and Pallé*, 2011].

3. Evidence of Scattered Sunlight

3.1. The Short-Wavelength Tail of the Spectrum

[8] Model predictions for $e \sim 0.34°$ and a broad range of aerosol loadings show that the spectrum of sunlight directly

[1]Instituto de Astrofísica de Canarias, La Laguna, Spain.
[2]Departamento de Astrofísica, Universidad de La Laguna, La Laguna, Spain.
[3]Centro de Astrobiología, CSIC-INTA, Madrid, Spain.

0094-8276/11/2011GL047981

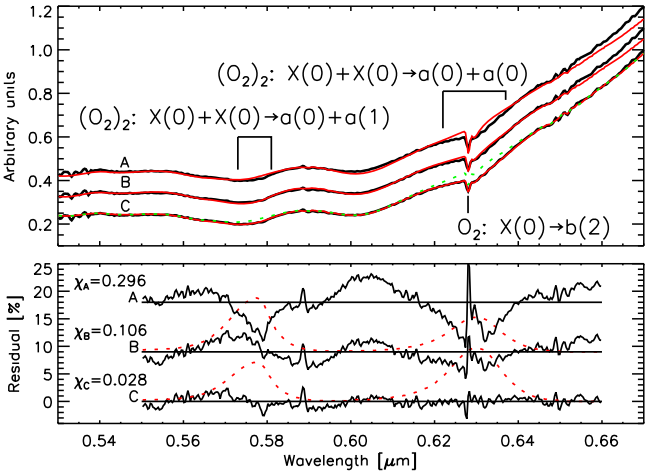

Figure 1. (top) Best fits (red) to the measured spectrum (black) from 550 to 660 nm. The dotted green line are the best fits divided by exp $(-\tau_{(O2)2})$. The comparison of the dotted and solid curves makes explicit the contributions from the coincidental in position, albeit distinct in nature, O_2 $X(0)\rightarrow b(2)$ and $(O_2)_2$ $X(0) + X(0)\rightarrow a(0) + a(0)$ absorption bands near 630 nm. (bottom) Fit residuals. For B and C, the dotted red curves are the $(O_2)_2$ contributions. In C, we infer an optimal ratio for the 577:630 nm integrated columns of ~1:2.

transmitted through the atmosphere is typically 2–3 orders of magnitude fainter at 400 nm than at 600 nm [*García Muñoz and Pallé*, 2011]. This is at odds with the eclipse data, which show that the measured spectrum is roughly flat to within a factor of 2 shortwards of 600 nm and that the fluxes at 400 and 880 nm are in a ratio of ~1:20. It thus means that direct sunlight is not the only contributor to the measured spectrum. *García Muñoz and Pallé* [2011] note that a flat spectrum at short wavelengths indicates that diffuse sunlight dominates locally over direct sunlight.

3.2. The $(O_2)_2$ Bands at 577 and 630 nm

[9] We fitted synthetic curves of the form $\Pi_i \exp(-\tau_i)$ to the measured spectrum from 550 to 660 nm. The curves include absorption by H_2O, O_3, O_2 and the $(O_2)_2$ collisional complex. One term, $\tau_{\rm cont} = \Sigma_{k=0}^{4} c_k (\lambda_*/\lambda)^k$, with $\lambda_* = 600$ nm, accounts for a continuum baseline. Thus, each curve contains up to ten degrees of freedom, namely, five c_k's, integrated columns for H_2O, O_3 and O_2, and, optionally, one integrated column for each of the $[X^3\Sigma_g^-(0)]_2\rightarrow a^1\Delta_g(0) + a^1\Delta_g(1)$ and $[X^3\Sigma_g^-(0)]_2\rightarrow[a^1\Delta_g(0)]_2$ bands of $(O_2)_2$ that occur at 577 and 630 nm, respectively. For the temperature-dependent gas properties, the temperature was fixed at 225 K. The synthetic curves were properly degraded and resampled. $m_j\,(1 - I_{\rm fit}\,(\lambda_j)/I_{\rm exp}\,(\lambda_j))^2$, where $I_{\rm fit}$ and $I_{\rm exp}$ are the synthetic and observed data, outputs the best fit parameters.

[10] Figure 1 summarizes the best fits obtained from three separate strategies, each of them treating the 577 and 630 nm bands of $(O_2)_2$ in a different manner. Strategy A fits the spectrum with null amounts of $(O_2)_2$; B includes $(O_2)_2$ and assumes the same integrated column for the two bands; and C allows for separate integrated columns for each of the 577 and 630 nm bands. In Figure 1 (top), the solid black curves represent the measured spectrum, shifted in the vertical for comparison with the synthetic curves. The red solid curves are the respective A, B and C best fits. Figure 1 (bottom) displays the residuals. Including $(O_2)_2$ reduces notably the fit residuals. The fit improves further if the integrated column at 630 nm is about twice the column at 577 nm. The latter conclusion is the core of the second argument that proves the significance of diffuse sunlight in the measured lunar eclipse spectrum. Some comments on the robustness of the fitting procedure can be found in the auxiliary material.[1]

[11] Taking C as the optimal strategy, the conclusion is that average sunlight photons at 577 and 630 nm follow different paths in the atmosphere. The direct trajectories of sunlight rays are dictated by the atmospheric refractive index, which does not change appreciably within such a narrow spectral interval. The amount of sunlight directly transmitted does however vary sharply with wavelength. Direct sunlight is more attenuated at 577 nm than at 630 nm due to the $\sim\lambda^{-4}$ behaviour of the Rayleigh cross section and the closer proximity of the 577 nm band to the absorption peak of the O_3 Chappuis band.

[12] We thus have to invoke sunlight scattered at the Earth's terminator to explain the measured spectrum. *García Muñoz and Pallé* [2011] show that in a lunar eclipse the bulk of diffuse sunlight near 600 nm originates from above 15 km. In the stratosphere, the $(O_2)_2$ density, which drops with a scale height half that of the background density, is negligibly small. Foreseeably, the signature of the $(O_2)_2$ bands in the diffuse sunlight spectrum is weak.

4. Analysis and Discussion

[13] Next, we generate model lunar eclipse spectra that reproduce the measured spectrum if a few reasonable assumptions on the loading and properties of airborne aerosols are introduced. The spectra, generated with the model described by *García Muñoz and Pallé* [2011], contain both direct and diffuse components. Further details on the underlying model assumptions can be found in the auxiliary material.

[14] The tracing of the direct sunbeam that reached the parcel of the Moon's disk tracked by the telescope reveals that the sunbeam intercepted the volcanic cloud formed in the Kasatochi eruption, as seen in Figure 2. It is expected that the direct sunlight component is more strongly affected by the volcanic cloud than the diffuse one, which originates from all terminator locations. This distinction is accounted for in the generation of the model spectra by assuming separate atmospheres for the calculation of each component.

[15] For simplicity, the model spectra are allowed only four adjustable parameters. These are $f_{\gamma 0}$, α' and f_{O_3} for the direct sunlight component, and $r_{\rm eff}$ for the diffuse one. In the former, $f_{\gamma 0}$ scales the reference aerosol extinction profile at 1.02 μm, α' is the Ångström exponent to extrapolate the 1.02-μm extinction profile to shorter wavelenghts, and f_{O_3} scales the reference ozone profile. In the calculation of the diffuse sunlight component, $r_{\rm eff}$ stands for a mean effective radius for aerosols at the terminator. The sulfate droplets of background aerosols in the quiescent atmosphere have $r_{\rm eff} \sim$ 0.1–0.2 μm, whereas volcanic ash particles with residence times longer than a few days may have $r_{\rm eff}$'s of a few

[1] Auxiliary materials are available in the HTML. doi:10.1029/2011GL047981.

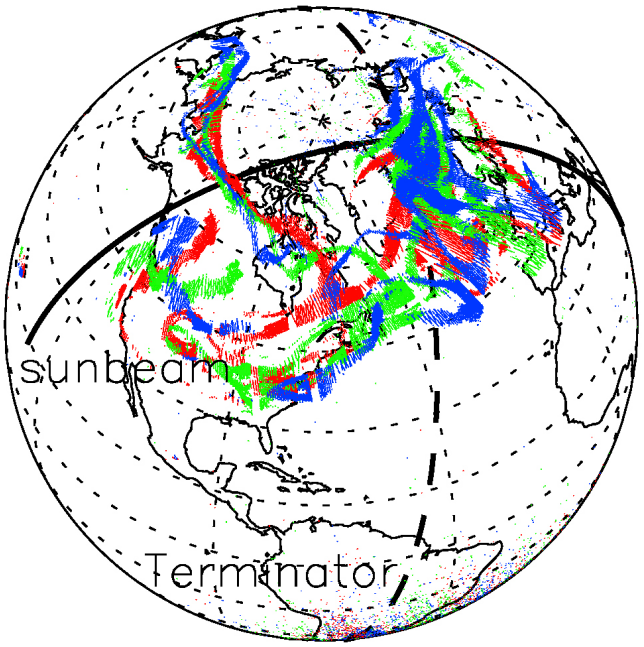

Figure 2. Solid: Projected mid-section trajectory of the sunbeam that reaches the lunar disk targeted by the telescope at 21:36UT on 16 August 2008. Overplotted, the SO_2 cloud (a usual volcanic cloud tracer) on 15, 16 and 17 August (red, green and blue, respectively) according to AURA/OMI data (downloaded from the Giovanni online data system, developed and maintained by the NASA GES DISC). The sunbeam's closest approach to the Earth's surface occurs in the North Atlantic region. The local tropopause is at ~10 km. Dashed: Line of the terminator.

microns [*Bauman et al.*, 2003; *Muñoz et al.*, 2004]. *Sioris et al.* [2010] report $r_{\rm eff}$'s of ~0.6 μm for September 2008, which are indicative of a perturbed atmosphere. It is unclear what the mean $r_{\rm eff}$ at the terminator was one week after the eruption. Thus, we explored a set of $r_{\rm eff}$ from 0.1 to 2 μm to bracket possible sizes. A large $r_{\rm eff}$ results in phase functions strongly peaked in the forward direction.

[16] For each $r_{\rm eff}$, one diffuse sunlight spectrum was produced. For each diffuse spectrum an algorithm seeks the $f_{\gamma 0}$, α' and f_{O_3} values producing the best fit of the direct + diffuse model spectra to the continuum of the measured spectrum. The algorithm forces the (flux-uncalibrated) measured spectrum to match the model spectra at 875 nm. Figure 3 shows the best fit for $r_{\rm eff}$ = 0.5 μm and the values inferred for the other three adjustable parameters. The *a* parameter is the multiplicative factor to pass from the normalization in the graph to the Earth-to-Sun ratio as discussed by *García Muñoz and Pallé* [2011]. Figure S1 in the auxiliary material shows the best fits for the full $r_{\rm eff}$ set. It is apparent the good *a posteriori* match of the O_2 bands in all cases. The differences between the measured spectrum and the best fits are of a few percent longwards of 600 nm, but of ~50% near 500 nm. This is a consequence of fitting the measured spectrum with models that contain a reduced number of adjustable parameters. The residuals longwards of 700 nm are mainly due to a known instrumental issue of uncorrected fringing.

[17] The $f_{\gamma 0}$ values inferred point to heavy aerosol loadings with peak extinctions of ~10^{-2} km^{-1} in the atmosphere intercepted by the direct sunbeam. Comparable extinctions were reported on global scales for a few months after the Pinatubo eruption [*Bauman et al.*, 2003]. Exponents α' ~ 0–0.15 are indicative of large-size particles being carried in the volcanic cloud. The conversion from SO_2 to sulfate droplets has an e-folding time of 20–50 days [*Kristiansen et al.*, 2010]. It is unlikely that one week after the eruption is enough time for large sulfate droplets to form. Thus, the α' values inferred suggest that the volcanic cloud carried sizeable amounts of unsedimented ash. *Sioris et al.* [2010] report small Ångström exponents of ~0.5 in early September 2008.

[18] The inset of Figure 3 shows the two component spectra near 600 nm. The diffuse spectrum is roughly flat and shows no evidence of $(O_2)_2$ absorption. When the direct and diffuse model spectra are added, the 577 nm band becomes more diluted than the 630 nm band, which translates into an effective integrated column at 630 nm larger than at 577 nm. For the case in Figure 3 the ratio is ~1:1.4, somewhat smaller than the ~1:2 ratio inferred from the measured spectrum. One may generally state that comparable amounts of direct and scattered sunlight near 600 nm lead to larger $(O_2)_2$ columns at the longer-wavelength band.

[19] Figure S1 in the auxiliary material proves that good fits to the measured spectrum are possible for the full $r_{\rm eff}$ set.

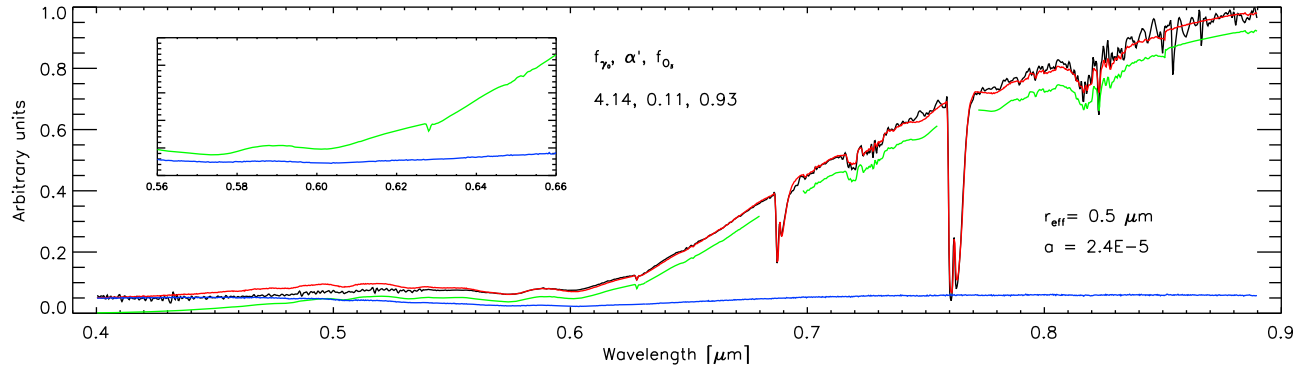

Figure 3. Best model fit for $r_{\rm eff}$ = 0.5 μm (red) to the measured spectrum (black). The model spectrum contains contributions from direct sunlight (green) and diffuse sunlight (blue). The inset is a zoom of the region near 600 nm. The algorithm aims the fit of the continuum away from O_2 and H_2O bands. The H_2O bands were fitted separately after the fit to the continuum. Figure S1 in the auxiliary material shows the best fits for the full set of $r_{\rm eff}$ values.

This means that the measured spectrum accepts one quantitative interpretation for each r_{eff}. In qualitative terms, though, the picture that we obtain is fairly consistent and indicates that the direct sunbeam was substantially attenuated by the volcanic cloud, which leads to an enhanced contrast of the diffuse component. For future efforts, we suggest that the flux calibration of the undivided spectra might help break the degeneracy.

[20] A comment is to be made regarding the Ring effect and the structure seen in the measured spectrum shortwards of 540 nm. The Ring effect refers to the smearing of solar Fraunhofer lines that occurs in the spectrum of sunlight scattered in the atmosphere [*Grainger and Ring*, 1962]. In the Earth's atmosphere, the Ring effect is due to rotational Raman scattering by N_2 and O_2 [*Kattawar et al.*, 1981]. Raman scattering redistributes in wavelength part of the incident photons, the redistribution being more evident where the incident solar spectrum shows the sharpest lines. The ratio of scattered to unscattered sunlight spectra reveals the Ring effect as a filling-in of the solar line cores. The detection of the Ring effect in the eclipse data would mean a further confirmation of scattered sunlight. The measured lunar eclipse spectrum shows that ripples do occur in the Fraunhofer region. The sign of the structures is however inverted with respect to what the Ring effect would produce. The inspection of the undivided umbra spectrum shows that the solar lines are unexpectedly deep, probably due to the limitation in the subtraction of the sky spectrum at these wavelengths, where the signal-to-noise ratio is the lowest. Thus, the structure seen in the measured spectrum cannot be attributed to the Ring effect. Further, a few quantitative arguments allow us to deem as minor the impact of the Ring effect on the measured lunar eclipse spectrum. Following *Kattawar et al.* [1981], the filling-in for forward-scattered sunlight is ~2.5% of the continuum Rayleigh-scattered by the gas. In the conditions explored here the filling-in would be undetectably small because the sunlight scattered by the gas contributes less than a few percent to the net sunlight scattered by gas and aerosols together.

[21] Pyrocumulonimbus (pyroCbs) is a recently-coined term to designate convective activity triggered or sustained by wildfires [*Fromm et al.*, 2010]. In extreme events, pyroCbs inject smoke and biomass-burning particles into the troposphere and lower stratosphere and alter the global aerosol loading. PyroCbs may result in aerosol extinctions $\sim 10^{-3}$–10^{-2} km^{-1} well above the tropopause, opacities that are often associated with volcanic clouds. It would be difficult to differentiate the impact on the eclipsed Moon of one such event from that of a volcanic eruption. To our knowledge, no extreme pyroCbs were reported in the weeks preceding the eclipse, a period that was monitored with unprecedented detail. Thus, if any, the contribution in the eclipse of pyroCbs blended with that of the Kasatochi cloud.

[22] The Perseids is one of the most copious meteor showers, running yearly from late July to late August. In 2008, its peak of activity occurred near 13 August. Despite recent work [*Mateshvili et al.*, 1999; *Renard et al.*, 2010], there are significant uncertainties on the optical properties of the atmosphere perturbed by meteor showers. *Mateshvili et al.* [1999] report two-fold enhancements with respect to pre-shower values in the twilight brightness above 20 km during the Leonids in 1998. Assuming that both meteor showers are comparable and that the brightness enhancement translates into a similar increase in stratospheric opacity, the effect of extraterrestrial dust would be more than one order of magnitude smaller than that by the volcanic perturbation. Thus, the effect of meteoroid dust in the measured spectrum is likely masked by the volcanic perturbation.

[23] We have shown that the lunar eclipse spectrum published by *Pallé et al.* [2009] was affected by sunlight scattered at the Earth's terminator. We offered theoretical arguments that hint at the Kasatochi eruption as the most plausible origin for the atmospheric perturbation needed to explain the observations. Future observations will allow us to compare lunar eclipse spectra obtained in different atmospheric conditions. In a broader context, it is worth mentioning that the retrieval of globally-averaged atmospheric optical properties is a relevant exercise towards the future characterization of transiting Earth-like extrasolar planets. As a corollary, we may state that the color of the lunar disk in umbra during the 16 August 2008 lunar eclipse was partly caused by diffuse sunlight.

[24] **Acknowledgments.** ELM acknowledges a Visiting Research Professorship at the Department of Geological Sciences of the University of Florida. We thank the two reviewers for constructive comments.

[25] The Editor thanks Chris Sioris and an anonymous reviewer for their assistance in evaluating this paper.

References

Bauman, J. J., P. B. Russell, M. A. Geller, and P. Hamill (2003), A stratospheric aerosol climatology from SAGE II and CLAES measurements: 2. Results and comparisons, 1984–1999, *J. Geophys. Res.*, *108*(D13), 4383, doi:10.1029/2002JD002993.

Fromm, M., D. T. Lindsey, R. Servranckx, G. Yue, T. Trickl, R. Sica, P. Doucet, and S. Godin-Beekmann (2010), The untold story of pyrocumulonimbus, *Bull. Am. Meteorol. Soc.*, *91*, 1193–1209.

García Muñoz, A., and E. Pallé (2011), Lunar eclipse theory revisited: Scattered sunlight in both the quiescent and the volcanically perturbed atmosphere, *J. Quant. Spectrosc. Radiat. Transfer*, *112*, 1609–1621.

Grainger, J. F., and J. Ring (1962), Anomalous Fraunhofer line profiles, *Nature*, *193*, 762.

Kattawar, G. W., A. T. Young, and T. J. Humphreys (1981), Inelastic scattering in planetary atmospheres. I. The Ring effect, without aerosols, *Astrophys. J.*, *243*, 1049–1057.

Keen, R. (1983), Volcanic aerosols and lunar eclipses, *Science*, *222*, 1011–1013.

Kristiansen, N. I., et al. (2010), Remote sensing and inverse transport modeling of the Kasatochi eruption sulfur dioxide cloud, *J. Geophys. Res.*, *115*, D00L16, doi:10.1029/2009JD013286.

Link, F. (1962), Lunar eclipses, in *Physics and Astronomy of the Moon*, edited by Z. Kopal, pp. 161–229, Academic, New York.

Martinsson, B. G., C. A. M. Brenninkmeijer, S. A. Carn, M. Hermann, K.-P. Heue, P. F. J. van Velthoven, and A. Zahn (2009), Influence of the 2008 Kasatochi volcanic eruption on sulfurous and carbonaceous aerosol constituents in the lower stratosphere, *Geophys. Res. Lett.*, *36*, L12813, doi:10.1029/2009GL038735.

Mateshvili, N., G. Mateshvili, I. Mateshvili, L. Gheondjian, and O. Avsajanishvili (1999), Vertical distribution of dust particles in the Earth's atmosphere during the 1998 Leonids, *Meteorit. Planet. Sci.*, *34*, 969–973.

Muñoz, O., H. Volten, J. W. Hovenier, B. Veihelmann, W. J. van der Zande, L. B. F. M. Waters, and W. I. Rose (2004), Scattering matrices of volcanic ash particles of Mount St. Helens, Redoubt, and Mount Spurr volcanoes, *J. Geophys. Res.*, *109*, D16201, doi:10.1029/2004JD004684.

Pallé, E., M. R. Zapatero Osorio, R. Barrena, P. Montañés-Rodríguez, and E. L. Martín (2009), Earth's transmission spectrum from lunar eclipse observations, *Nature*, *459*, 814–816.

Renard, J.-B., G. Berthet, V. Salazar, V. Catoire, M. Tagger, B. Gaubicher, and C. Robert (2010), In situ detection of aerosol layers in the middle stratosphere, *Geophys. Res. Lett.*, *37*, L20803, doi:10.1029/2010GL044307.

Sioris, C. E., C. D. Boone, P. F. Bernath, J. Zou, C. T. McElroy, and C. A. McLinden (2010), Atmospheric Chemistry Experiment (ACE) observations of aerosol in the upper troposphere and lower stratosphere from

the Kasatochi volcanic eruption, *J. Geophys. Res.*, *115*, D00L14, doi:10.1029/2009JD013469.

Ugolnikov, O. S., and I. A. Maslov (2008), Altitude and latitude distribution of atmospheric aerosol and water vapor from the narrow-band lunar eclipse photometry, *J. Quant. Spectros. Radiat. Transfer*, *109*, 378–388.

Vidal-Madjar, A., et al. (2010), The Earth as an extrasolar transiting planet. Earth's atmospheric composition and thickness revealed by lunar eclipse observations, *Astron. Astrophys.*, *523*, A57.

Vollmer, M., and S. D. Gedzelman (2008), Simulating irradiance during lunar eclipses: The spherically symmetric case, *Appl. Opt.*, *47*, H52–H61.

Waythomas, C. F., W. E. Scott, S. G. Prejean, D. J. Schneider, P. Izbekov, and C. J. Nye (2010), The 7–8 August 2008 eruption of Kasatochi Volcano, central Aleutian Islands, Alaska, *J. Geophys. Res.*, *115*, B00B06, doi:10.1029/2010JB007437.

A. García Muñoz and E. Pallé, Instituto de Astrofísica de Canarias, C/Vía Láctea s/n, E-38200 La Laguna, Spain. (agm@iac.es)

E. L. Martín and M. R. Zapatero Osorio, Centro de Astrobiología, CSIC-INTA, Ctra. de Torrejón a Ajalvir, km 4, E-28550 Madrid, Spain.